

1 Thermal Evaluation of Sustainable Asphalt Pavements with Energy 2 Harvesting Purposes

3 Jose L. Concha¹, Jose Norambuena-Contreras², Eric Aguilera³

4 (¹ LabMAT, Department of Civil and Environmental Engineering, University of Bío-Bío,
5 Concepción, Chile, jlconcha@ubiobio.cl)

6 (² LabMAT, Department of Civil and Environmental Engineering, University of Bío-Bío,
7 Concepción, Chile, jnorambuena@ubiobio.cl)

8 (³ LabMAT, Department of Civil and Environmental Engineering, University of Bío-Bío,
9 Concepción, Chile, eraguile@alumnos.ubiobio.cl)

10 ABSTRACT

11 This paper presents the influence of metallic waste addition on the thermal behaviour of
12 asphalt mixtures and their use as a solar collector. With this purpose, different asphalt mixtures
13 with the same aggregates gradation and bitumen content but with two different types of metallic
14 waste, steel shavings and steel wool fibres, were experimentally analysed. Thermophysical and
15 heating properties of asphalt specimens with, and without, metallic waste were evaluated.
16 Furthermore, thermal behaviour of a solar collector prototype was evaluated under different solar
17 irradiance conditions. The main results showed that the addition of steel fibres improved the
18 thermal conductivity and thermal diffusivity of asphalt mixtures and that steel fibres were more
19 efficient than steel shavings in the heat transfer process through the mixtures. Finally, it was proven
20 that the developed solar collector was able to transfer heat from the pavement surface to the water
21 flowing inside it, and that the water reached a temperature of 53°C under the maximum irradiance
22 conditions. Therefore, it was proven that metallic waste can be potentially used to develop new
23 sustainable asphalt pavements with energy harvesting purposes.
24

25 **Keywords:** Asphalt mixture; Metallic waste; Thermal performance; Solar collector.

26 1. INTRODUCTION

27 Recent studies indicate that countries in South America have some of the highest solar
28 radiation levels in the world, with average values of Global Horizontal Irradiance (GHI) over 7
29 kWh/m² and Direct Normal Irradiance (DNI) over 9 kWh/m² [1]. In the right conditions, these
30 radiation levels can increase the temperature of asphalt pavements up to 60°C [2]. Thus, the heat
31 absorbed by asphalt pavements can be used with energetic purposes, making them asphalt solar
32 collectors [[3],[4]]. This technology consists on the embedment of pipes inside the pavement with
33 a fluid circulating through them [5], and two of their main applications are: thermal comfort of
34 adjacent buildings and de-icing systems [2].

35 According to Mallick et al. [3], the performance of asphalt solar collectors is based on the
36 solar radiation absorption capacity of the pavement, which increases its surface temperature. This
37 way, the absorbed heat can be transferred to the circulating flow. In this context, Hassn et al. [6]
38 stated that the pavement surface temperature depends on heat transfer mechanisms, such as:
39 radiation, convection and conduction. However, variables like the porosity of asphalt mixture [7]
40 and the thermal properties of its components can also have influence [8]. From a practical
41 viewpoint, asphalt pavements can be good solar radiation absorbers, because of their black colour

1 and high absorptivity. But they also have high emissivity [4], which can reduce the efficiency of
2 an asphalt solar collector. To solve this, recent studies concluded that the addition of metallic waste
3 in asphalt mixtures can: 1) improve their heating properties [[9],[10]], 2) increase their thermal
4 conductivity counteracting the pavement emissivity [[5],[8]], and 3) reduce the contribution of
5 pavements to the urban heat-island effect [11], efficiently transferring heat from the pavement
6 surface to the fluid in the asphalt solar collector.

7 The aim of this study was to analyse the influence of the type and content of metallic waste
8 on the thermal behaviour of asphalt mixtures and their use as solar radiation absorbent material.
9 With this purpose, 1) the thermophysical properties of asphalt mixtures with metallic fibres and
10 shavings and 2) the performance of an experimental prototype of asphalt solar collector, were
11 evaluated.

12 2. MATERIALS AND METHODS

13 2.1 Materials

14 A standard dense asphalt mixture was used in the study. The aggregates were classified in
15 three fractions: coarse (size: 5-12.5 mm, density: 2.779 g/cm³), fine (size: 0.08-5 mm, density:
16 2.721 g/cm³) and filler (size <0.08 mm, density: 2.813 g/cm³). The bitumen used was a CA-24
17 with a penetration grade of 80/100 mm at 25°C and density 1.039 g/cm³. Also, steel fibres and
18 shavings were added. Fibres were made of low-carbon steel with density 7.180 g/cm³, average
19 diameter of 0.157 mm, average aspect ratio of 30 and initial length range 2-8 mm. In contrast,
20 shavings were made of austenitic stainless steel with density 7.980 g/cm³, average thickness of
21 0.335 mm and initial length range 1-6 mm. Steel waste (M_w) were added to the mixtures in 4
22 percentages: 2%, 4%, 6% and 8%, by total volume of bitumen. Finally, 1 reference mixture, 4
23 mixtures with fibres and 4 mixtures with shavings were manufactured, using the same aggregates
24 gradation and bitumen content.

26 2.2 Preparation of asphalt specimens

27 Cylindrical Marshall specimens with 100 mm-diameter and 60 mm-height were
28 manufactured. To prepare the test specimens, the aggregates were previously heated at 150°C for
29 24 h, while the bitumen and metallic waste were heated at 150°C for 2 h. Then, raw materials were
30 mixed for 3.5 min in a laboratory planetary mixer at a rate of 100 rpm, keeping a constant
31 temperature of 150°C. They were added in the following order: bitumen and metallic waste, coarse
32 aggregate, fine aggregate and filler. Then, each batch of asphalt mixture was poured into a Marshall
33 mould and compacted with a Marshall hammer applying 75 blows on each face of the specimen.
34 A total of 32 specimens with metallic waste and 4 reference specimens were manufactured.

36 2.3 Bulk density and air void content

37 Bulk density of each specimen was calculated as the ratio between the dry mass and the
38 real volume obtained as the water-submerged mass. In addition, the Air Void Content (AVC) was
39 determined using the previous calculation of the bulk density and the theoretical maximum density
40 according to Eq. (1).

$$41 \text{AVC}(\%) = (\rho_{mt} - \rho_a) / \rho_{mt} \quad (1)$$

1 Where ρ_a and ρ_{mt} are the bulk density and the theoretical maximum density of each
2 mixture in g/cm^3 , respectively. Representative values of ρ_a and AVC for each mixture were
3 calculated as the average value of 3 measurements.
4

5 **2.4 Thermophysical properties of asphalt mixtures**

6 To evaluate the influence of the type and content of metallic waste on the thermophysical
7 properties of the asphalt specimens with and without metallic waste, thermal conductivity (λ),
8 specific heat (C_p) and thermal diffusivity (β) were determined. First, λ was measured using the
9 KD2-Pro thermal properties analyser (Decagon Devices) formed of a handheld controller and a
10 needle stainless steel RK-1 sensor (length of 60mm and diameter of 3.9mm), with a measurement
11 range of $0.1\text{-}6.0 \text{ Wm}^{-1}\text{K}^{-1}$. All the measurements were made based on the transient linear heat
12 source theory [12]. Additionally, C_p was calculated according to Eq. (2). Where m_T is the total
13 mass of each asphalt specimen in kg; m_{Ag} , m_M and $m_{M.W}$, and C_{Ag} , C_M and $C_{M.W}$, are the mass in
14 kg and the specific heat in J/kgK of aggregates, bitumen and and metallic waste, respectively.
15 $C_{M.W}$ was differentiated as C_f or C_s in the case of fibres and shavings, respectively. C_{Ag} [7], C_M ,
16 C_f [8] and C_s [13] values were 908 J/kgK , 1900 J/kgK , 482 J/kgK and 450 J/kgK , respectively.
17

$$18 \quad C_p = (m_{Ag} * C_{Ag} + m_M * C_M + m_{M.W} * C_{M.W})/m_T \quad (2)$$

$$19 \quad \beta = \lambda/(\rho_a * C_p) \quad (3)$$

20 Finally, β was calculated according to Eq. (3). Where λ was measured in W/mK , ρ_a in
21 g/cm^3 and C_p of each mixture in J/kgK .
22

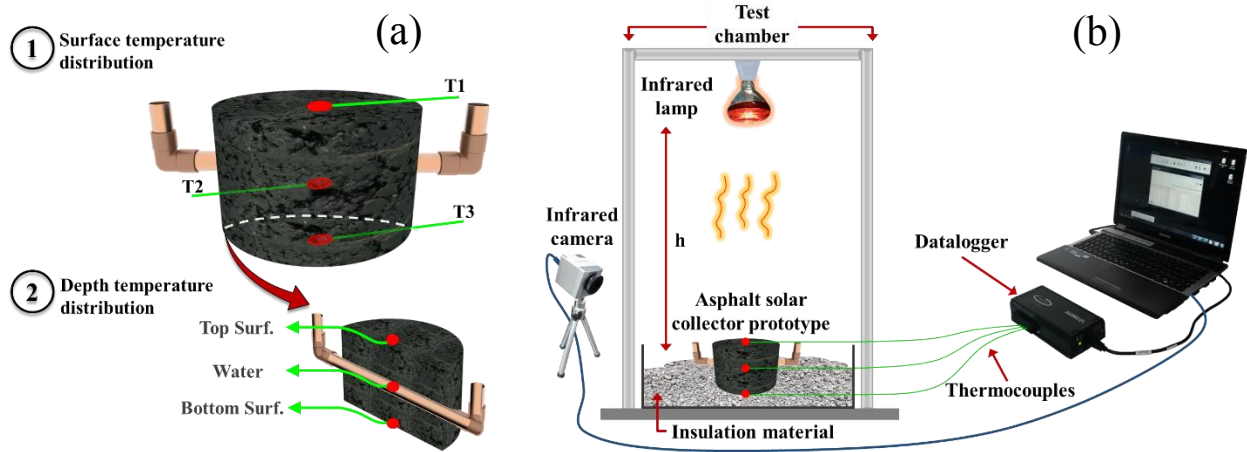
23 **2.5 Solar irradiance simulation in laboratory**

24 To simulate solar irradiance in laboratory conditions, radiation data in the city of
25 Concepción (Chile), between 2001 and 2013 were statistically analysed. The maximum and
26 minimum average solar irradiance conditions were determined from the analysis, being
27 respectively 898.57 W/m^2 in December (summer season), and 289.38 W/m^2 in June (winter
28 season). Then, those values were used as input parameters on the solar model developed by
29 Norambuena-Contreras et al. [14], to estimate the needed height at what a 250W infrared radiation
30 source should be placed to simulate a specific solar irradiance. Consequently, the calculated
31 distances between the radiation source and the asphalt specimen to simulate the conditions of
32 maximum and minimum solar irradiance were 0.4 m and 0.9 m, respectively.
33
34
35

36 **2.6 Thermal behaviour of asphalt mixtures and solar collector under infrared radiation**

37 To evaluate the thermal behaviour of asphalt mixtures, each specimen was exposed to a
38 250W infrared radiation source that simulated the conditions of maximum and minimum
39 irradiance estimated in section 2.5. To do this, temperature was measured in steady-state
40 conditions during 24 h, and in transient-state conditions during 12 h-heating and 12 h-cooling.
41 Furthermore, to evaluate the thermal behaviour of an asphalt solar collector prototype, one
42 specimen with metallic waste was selected, and a 12 mm-diameter copper pipe was installed inside
43 it, with a water storage capacity of 20 cm^3 , see Figure. 1(a). The prototype was also exposed to the
44 250 W infrared radiation source simulating the maximum and minimum solar irradiance. The
45 temperature in the solar collector was measured in transient-state conditions during 12 h heating

1 and 12 h cooling, thus simulating a day-night cycle. Both in the cases of asphalt specimens and
 2 the solar collector, the temperature distribution was registered using 3 K-type thermocouples, and
 3 the surface temperature was registered using an infrared camera Optris PI160, Figure, 1(b) and (b).



4
 5 **FIGURE 1** Scheme of (a) asphalt solar collector and thermocouples distribution, and (b)
 6 heating test in asphalt mixtures and solar collector via infrared radiation.

7 **3. RESULTS AND DISCUSSION**

8 **3.1 Influence of metallic waste on the thermophysical properties of asphalt mixtures**

9 Table 1 presents the average results of the thermophysical properties of asphalt mixtures
 10 with, and without, metallic waste. It can be observed that the addition of metallic waste reduced
 11 the bulk density of the mixtures, compared to mixtures without waste, which was due to the
 12 increase of their porosity. Likewise, an increase on the porosity of asphalt mixtures can affect their
 13 thermophysical properties and the collector efficiency. Specifically, an increase of λ in asphalt
 14 mixtures can allow the collector to transfer more energy to the fluid inside it. However, results
 15 showed a reduction of this property with the increase of the amount of metallic waste, which was
 16 attributed to the increase of mixtures porosity, see Table 1. Moreover, λ values were higher in
 17 mixtures with fibres than in those with shavings, because of 2 reasons: 1) the high aspect ratio of
 18 the fibres that generate more contact points between them, and 2) the different value of λ for each
 19 metallic waste [15].
 20

21 **TABLE 1** Average results of thermophysical properties in asphalt mixtures.

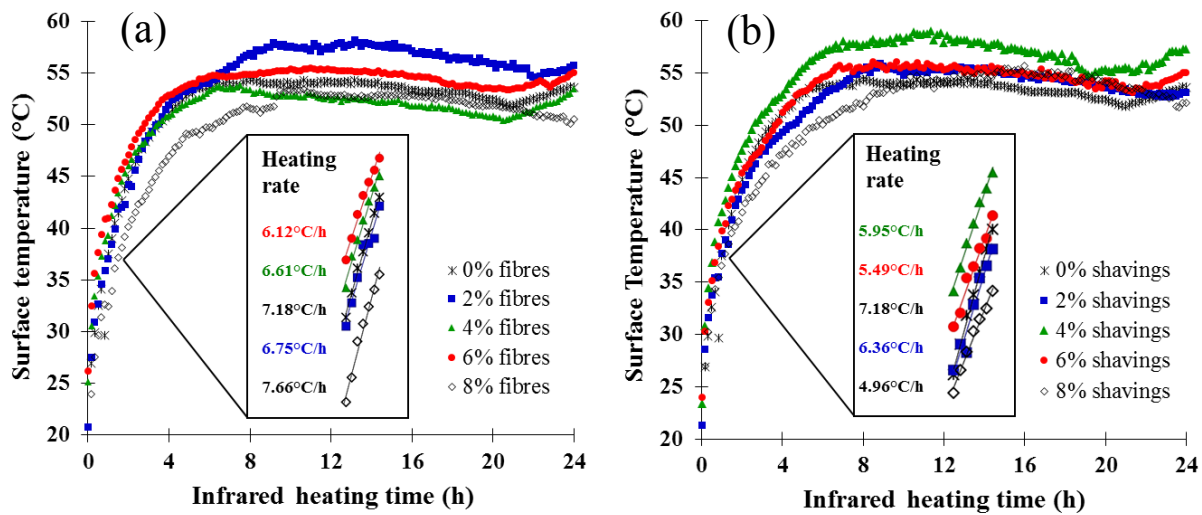
M_w	Steel wool fibres					Steel shavings				
	ρ_a (g/cm ³)	AVC (%)	λ (W/mK)	C_p (J/kgK)	β ($\times 10^{-7}$) (m ² /s)	ρ_a (g/cm ³)	AVC (%)	λ (W/mK)	C_p (J/kgK)	β ($\times 10^{-7}$) (m ² /s)
2%	2.347	6.86	1.343	954.67	5.994	2.362	6.26	1.187	954.01	5.268
4%	2.313	9.05	1.385	951.45	6.293	2.338	8.05	1.246	950.16	5.609
6%	2.342	8.24	1.379	948.27	6.209	2.316	9.27	1.257	946.36	5.735
8%	2.310	10.21	1.369	945.13	6.270	2.285	11.22	1.252	942.62	5.813
0%	2.356	5.83	1.406	957.93	6.230	2.356	5.83	1.406	957.93	6.230

22 Besides, the addition of metallic waste in asphalt mixtures slightly reduced C_p values (see
 23 Table 1), consequently decreasing the amount of energy needed to increase their temperature.
 24 Furthermore, the addition of metallic fibres mainly increased β with respect to a reference mixture,
 25

1 thus increasing the heat transfer rate inside asphalt mixtures. This was attributed to the fibres
 2 morphology. While the reduction of β in asphalt mixtures with shavings was associated with the
 3 increase on the porosity of the mixtures. Finally, due to the fact that: 1) higher values of λ increase
 4 the amount of heat transfer to low thermal energy zones [11], 2) lower values of C_p increase the
 5 heating rates of asphalt mixtures, and 3) higher values of β increase the heating rate through
 6 asphalt mixtures, the results indicated that asphalt mixtures with 4% of metallic fibres can be
 7 potentially used to develop an asphalt solar collector prototype.
 8

9 3.2 Heating properties of asphalt mixtures and solar collector under infrared radiation

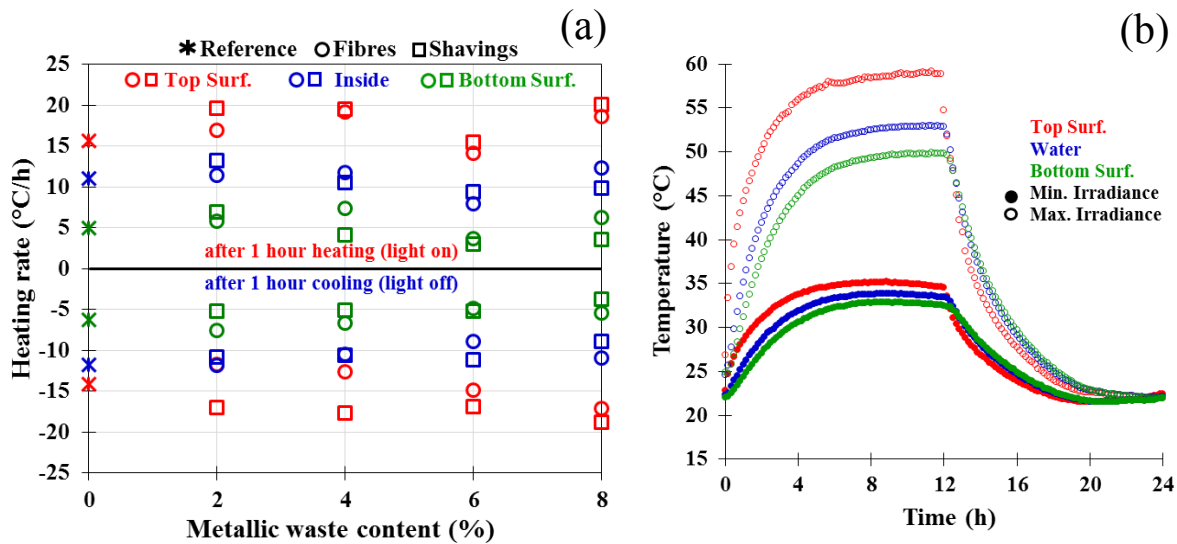
10 The heating results under steady-state conditions on asphalt mixtures with, and without,
 11 addition of fibres, see Figure. 2(a), and shavings, see Figure. 2(b), showed that there is no direct
 12 relationship between the temperature reached by the mixtures and the amount of metallic waste.
 13 This was attributed to the heterogeneous distribution of metallic waste inside the asphalt mixtures
 14 and to the increase of their porosity. In addition, Figure. 2 presents the results of heating rate
 15 between the 2nd and 3rd hours of exposition to infrared radiation, showing that the heating rate in
 16 mixtures with fibres was higher than that in mixtures with shavings. Hence, the morphology and
 17 distribution of steel wool fibres together with the improvement on the thermophysical properties
 18 of mixtures with fibres were the most influential variables during the first hours of heating.
 19



20
 21 **FIGURE 2 Temperature evolution under steady-state conditions in asphalt mixtures with:**
 22 **(a) steel fibres and (b) steel shavings.**
 23

24 Moreover, as shown in Figure. 2, the temperature of asphalt specimens after 12 h of heating
 25 kept constant reaching a steady state. However, the addition of metallic waste to asphalt mixtures
 26 did not contribute to improve this thermal balance, compared to a reference mixture without waste.
 27 In addition, Figure. 3(a) presents the heating rate on the top surface, inside and under the bottom
 28 surface of all asphalt mixtures after 1 h-heating and 1 h-cooling. In particular, a high heating rate
 29 can allow the fluid to reach higher temperatures in a specific time. While lower cooling rates allow
 30 the fluid to keep longer the reached temperature, thus increasing its efficiency. In this context,
 31 Figure. 3(a) shows that the amount of metallic waste added to the mixtures and the heating-cooling
 32 rate were no directly related. However, asphalt mixtures with 4% of steel fibres increased their
 33 heating rates and decreased their cooling rates with respect to mixtures without metallic waste.

1 Furthermore, Figure. 3(b) shows the heating results of an asphalt solar collector prototype
 2 made using an asphalt specimen with 4% of metallic fibres, under maximum and minimum
 3 irradiance conditions. It can be observed that there is a fast increase of temperature during the first
 4 4 h of heating, and that the collector reached the thermal balance after 6 h. However, the reached
 5 temperature was more stable in the minimum irradiance condition. This was attributed to the fact
 6 that the collector absorbed less thermal energy under the minimum irradiance conditions, thus
 7 reducing the effect of the fibres and the copper pipe on the heat transfer process through the
 8 mixture. Finally, after 12 h of heating, the water inside the collector reached temperatures of 33°C
 9 and 53°C, under the minimum and maximum solar irradiance conditions, respectively, which
 10 represented a temperature reduction of 3.32% and 10.23% with respect to that reached on the top
 11 surface of the collector.
 12



13 **FIGURE 3** Temperature evolution under transient-state conditions in: (a) reinforced
 14 asphalt mixtures and (b) asphalt solar collector prototype.
 15

16 **4. CONCLUSIONS**

- 17
- 18 • Density of asphalt mixtures with metallic waste reduced with the air voids content increase,
 19 that was mainly attributed to the total volume variation of each asphalt specimen, rather
 20 than the variation of the mass.
 - 21 • Thermal conductivity and specific heat of asphalt mixtures were reduced with the addition
 22 of metallic waste. However, the incorporation of steel wool fibres in asphalt mixtures
 23 caused an increase on their thermal diffusivity, consequently decreasing the influence of
 24 air voids on the heat transfer through the mixtures.
 - 25 • In addition, under steady-state heating, asphalt mixtures with fibres increased their heating
 26 rate during the first hours of exposition to infrared solar radiation. In contrast, under
 27 transient-state heating, just in the case of asphalt mixtures with 4% of fibres an increase on
 28 the heating rate and a decrease on the cooling rate was registered.
 - 29 • Finally, it was proven that the asphalt solar collector with 4% fibres was able to transfer
 30 heat from the pavement surface to the water flowing inside it, and that the water reached a
 temperature of 53°C under the maximum irradiance conditions.

1 5. ACKNOWLEDGMENTS

2 Authors want to thank the financial support given by the National Commission for
3 Scientific & Technological Research (CONICYT) from the Government of Chile, through the
4 Research Project FONDECYT Initiation 2014 N°11140103.

5 6. REFERENCES

- 6 [1] Watts D, Valdés M.F, Jara D, Watson A. Potential residential PV development in
7 Chile: the effect of net metering and net billing schemes for grid-connected PV systems,
8 *Renewable and Sustainable Energy Reviews*, 41, pp. 1037-1051. 2015.
- 9 [2] Bijsterveld W.T.V., Houben L.J.M., Scarpas A., Molenaar A.A.A. Using pavement
10 as solar collector: effect on pavement temperature and structural response, *Journal of*
11 *Transportation Research Board*, 1778, pp. 140-148. 2001.
- 12 [3] Mallick R.B., Chen B.L., Bhowmick S. Harvesting energy from asphalt pavements
13 and reducing the heat island effect, *International Journal of Sustainable Engineering*, 2:3, pp. 214-
14 228. 2009.
- 15 [4] Bobes-Jesus V., Pascual-Muñoz P., Castro-Fresno D., Rodriguez-Hernandez J.
16 Asphalt solar collectors: a literature review, *Applied Energy*, 102, pp. 962-970. 2013.
- 17 [5] Partl M. N., García A., Norambuena-Contreras J., Bueno M. Influence of steel wool
18 fibers on the mechanical, thermal, and healing properties of dense asphalt concrete, *Journal of*
19 *Testing and Evaluation*, 42(5), pp. 1-12. 2014.
- 20 [6] Hassn A., Chiarelli A., Dawson A., Garcia A. Thermal properties of asphalt
21 pavements under dry and wet conditions, *Materials & Design*, 91, pp. 432-439. 2016.
- 22 [7] Hassn A., Aboufoul M., Wu Y., Dawson A., Garcia A. Effect of air voids content
23 on thermal properties of asphalt mixtures, *Construction and Building Materials*, 115, pp. 327-335.
24 2016.
- 25 [8] Norambuena-Contreras J, García Á. Self-healing of asphalt mixture by microwave
26 and induction heating, *Materials & Design*, 106, pp. 404-414. 2016.
- 27 [9] Franesqui M.A, Yepes J, García-González C. Top-down cracking self-healing af
28 asphalt pavements with Steel filler from industrial waste applying microwaves, *Construction and*
29 *Building Materials*, 149, pp. 612-620. 2017.
- 30 [10] Norambuena-Contreras J. and Concha J.L. Self-Healing of Asphalt Mixtures Via
31 Microwave Heating, ISAP2016, Jackson Hole, Wyoming, USA. 2016.
- 32 [11] Mohajerani A, Bakaric J, Jeffrey-Bailey T. The urban heat island effect, its causes
33 and mitigation, with reference to the thermal properties of asphalt concrete, *Journal of*
34 *Environmental Management*, 197, pp. 522-538. 2017.
- 35 [12] ASTM D 5334, Standard Test Method for Determination of Thermal Conductivity
36 of Soil and Soft Rock by Thermal Needle Probe Procedure. American Society for Testing and
37 Materials, 2008.
- 38 [13] Technical Building Code [Código Técnico de la Edificación (CTE)]. Catálogo de
39 elementos constructivos del CTE, Spain, 2010.
- 40 [14] Norambuena-Contreras J, Concha J.L, Borinaga-Treviño R. Evaluation of the
41 thermophysical and heating properties of a composite rubber membrane with energy harvesting
42 purposes. *Polymer Testing*, 2017. doi: org/10.1016/j.polymertesting.2017.09.042
- 43 [15] Chagas G.M.P, Barbosa P.A, Barbosa C.A, Machado I.F. Thermal analysis of the
44 chip formation in austenitic stainless steel. *Procedia CIRP*; 8, pp. 293-298. 2013.